Photoionization of Phenolates and Scavenging of Hydrated Electrons by No_3^-: A Study of the Reaction Mechanism by FT-EPR

Alejandro Bussandri and Hans van Willigen*

Department of Chemistry, University of Massachusetts at Boston, Boston, Massachusetts 02125

Received: October 5, 2000; In Final Form: January 9, 2001

The mechanism of photoionization of phenol, *p*-cresol, and tyrosine in alkaline aqueous solution was investigated with Fourier Transform EPR. The spectra given by the phenoxyl radicals and hydrated electron (e_{aq}^-) display a low-frequency (high-field) absorption/high-frequency (low-field) emission (A/E) polarization pattern generated by radical pair mechanism chemically induced dynamic electron polarization (RPM CIDEP). Upon addition of nitrate the NO_3^{2-} radical is formed by capture of e_{aq}^-. With $[NO_3^-] < 10^{-2}$ M the three-line spectrum due to NO_3^{2-} shows a 1:1:1 absorption pattern reflecting spin polarization carried over from the hydrated electron. At high nitrate concentration, $[NO_3^-] > 5 \times 10^{-2}$ M, both the phenoxyl and NO_3^{2-} signals display an E/A polarization pattern at short delay times (<1 μs) between pulsed-laser excitation and microwave pulse. This is attributed to RPM CIDEP generated by the $[PhO^{\bullet}\cdots NO_3^{2-}]$ radical pair formed in the reaction $[PhO^{\bullet}\cdots e_{aq}^-] + NO_3^- \rightarrow [PhO^{\bullet}\cdots NO_3^{2-}]$. At longer delay times (>1 μs), the spin polarization pattern in the spectrum of NO_3^{2-} changes to A/E as a result of F-pair CIDEP produced by the back reaction $PhO^{\bullet} + NO_3^{2-} \rightarrow PhO^- + NO_3^-$. The experimental data show that the sign of the exchange interaction *J* between the unpaired electron in $[PhO^{\bullet}\cdots e_{aq}^-]$ is opposite to that in $[PhO^{\bullet}\cdots NO_3^{2-}]$. From the CIDEP effects, it can be concluded further that the photoionization must occur from a singlet excited state of the phenolates so that in the radical pair $[PhO^{\bullet}\cdots e_{aq}^-]$ *J* must have the positive sign.

1. Introduction

Earlier work carried out on phenol and substituted phenols has shown that the photochemical properties of these compounds are a sensitive function of reaction conditions.[1−9] Photoexcitation can lead to photoionization and/or O−H bond dissociation, and it is found that the relative importance of these two reaction paths depends on the solvent and, in aqueous solution, on the pH of the solution.[7] Furthermore, quantum yields in some cases display a pronounced dependence on excitation wavelength.[4−8]

In basic aqueous solution (pH > 10), photoexcitation of the phenolates initiates the electron ejection reaction[3,5,8]

$$PhO^- \xrightarrow{h\nu} [PhO^{\bullet}\cdots e_{aq}^-] \rightarrow PhO^{\bullet} + e_{aq}^- \qquad (1)$$

Photoionization at relatively low photon flux is a single-photon process.[5] With high power pulsed-laser excitation, a two-photon process may play a role as well.[3,10] The quantum yield of the electron ejection reaction was found to depend on the wavelength of excitation.[5,11] This effect was taken as evidence that the reaction is fast enough to compete with internal conversion and vibrational relaxation processes producing the fluorescent excited state.[5] Indeed, a picosecond transient optical absorption study of photoionization of phenol in basic aqueous solution shows that the hydrated electron is formed within the time span of the excitation pulse (~27 ps).[10] In general, transient absorption studies of the photoionization of organic molecules in aqueous solution have found it to be an ultrafast process,[12−16] that can generate solvated electrons in the subpicosecond time domain.[14−16]

The question of whether photoionization involves a singlet excited state and/or triplet state has not been settled definitively.[3,5,10,17,18] The interpretation of spectroscopic data generally is based on the premise that the reaction occurs from a singlet excited state.[5,10,17] However, some experimental evidence points to a mechanism that involves a triplet excited state.[3,18] In a number of studies, continuous wave (cw) time-resolved EPR (TREPR) and FT-EPR have been used to study the photoionization of phenols in alkaline aqueous solution in efforts to resolve the question of the reaction mechanism.[17−19] These studies are of interest because of the expectation that the question of the spin multiplicity of the reactive excited state can be answered by an analysis of Chemically Induced Dynamic Electron Polarization (CIDEP[20]) effects.[17−19]

In the TREPR study of photoionization of phenol and some substituted phenols by Jeevarajan and Fessenden,[17] it was found that the spectra given by the phenoxyl radicals and hydrated electron display a low-field emission/high-field absorption (E/A) spin polarization pattern. This CIDEP pattern is due to the spin state evolution during the lifetime of the radical pair $[PhO^{\bullet}\cdots e_{aq}^-]$ (geminate Radical Pair Mechanism (RPM) CIDEP[20]) and is determined by the spin multiplicity of the precursor excited state. According to RPM CIDEP theory,[21] if the exchange interaction (*J*) between the unpaired electrons in a radical pair is negative, i.e., the singlet radical pair state lies below that of the triplet state, an E/A polarization pattern points to a triplet excited state as the precursor of doublet radical products. On the other hand, if $J > 0$ an E/A pattern reflects a singlet excited-state precursor. In most photochemical reactions that produce a pair of doublet free radicals, it has been established that $J < 0$. However, in some cases, experimental evidence indicates that $J > 0$.[22] For this reason, the RPM CIDEP pattern alone does not constitute an unambiguous diagnostic of the spin state of the reactive excited state.

10.1021/jp0036590 CCC: $20.00
Published on Web 04/06/2001

In the case of the photoionization of phenols, Jeevarajan and Fessenden present evidence that the reaction must occur via the singlet excited state, i.e., $J > 0$ in the radical pair [PhO$^{\bullet}\cdots$e$^-_{aq}$].[17] In a TREPR study of the photoionization of tyrosine in alkaline solution, Clancy and Forbes[18] also found an E/A polarization pattern. However, these authors conclude from the results of triplet quenching experiments that the reaction involves a triplet excited-state reaction path ($J < 0$). A similar conclusion was reached in a FT-EPR study of the photoionization of 3,4-methylenedioxyphenol (sesamol) carried out in this laboratory.[19]

This report concerns the application of FT-EPR in the study of the formation and decay of free radicals generated by pulsed-laser excitation of alkaline solutions of phenol, *p*-cresol, and tyrosine. The FT-EPR spectra exhibit high spectral and time resolution and good signal-to-noise so that CIDEP effects could be analyzed quantitatively. With the aid of measurements of the effect of e$^-_{aq}$ scavenging by NO_3^- and published information on the kinetics of photoionization[10] it was established that the reaction occurs primarily via a singlet excited state of the phenols.

2. Experimental Section

Phenol (Aldrich, 98%) was purified by sublimation. Tyrosine (Ajinomoto Co.) and *p*-cresol (Aldrich, 99%) were used without further purification. Aqueous solutions with phenol concentrations of 10 mM were prepared with water from a Millipore Milli-Q purification system. The pH of the solutions was adjusted with KOH. Solutions, deoxygenated with argon gas, were pumped through a flat quartz cell held in the microwave cavity.

Samples were excited with 308 nm UV-light from a Lambda Physik EMG103 MSC XeCl excimer laser (~15 ns pulse width, 60 mJ pulse, repetition rate 40 Hz), 266 nm UV-light from a Quanta-Ray GCR-14S Nd:YAG laser (~8 ns pulse width, 10 mJ/pulse, repetition rate 10 Hz), or 193 nm UV-light from a Lambda Physik Compex 102 ArF excimer laser (~15 ns pulse width, 20 mJ/pulse, repetition rate 20 Hz).

FT-EPR measurements were carried out with the in-house-built instrument described before.[23] The response of the sample to the $\pi/2$ microwave pulse (~15 ns) was detected in quadrature with application of the CYCLOPS phase-cycling routine. Because spectra cover a frequency range exceeding the bandwidth of the spectrometer, they are assembled from data recorded with a range of field settings. FIDs were recorded for a series of delay times (10 ns $< \tau_d <$ 100 μs) between laser excitation and microwave pulse. For each field setting, the FIDs generally were the time average of signals generated by a total of 400 laser shots (266 nm, 193 nm) or 2000 laser shots (308 nm). Amplitudes, phases, and line widths of resonance peaks were derived from the FIDs with a LPSVD analysis routine.[24] Except where noted otherwise, all measurements were performed at room temperature.

3. Results

3.1. Photoionization of Phenolates. Figure 1(a−c) shows the FT-EPR spectra given by aqueous solutions (10 mM, pH 11) of phenol, tyrosine, and *p*-cresol for a delay of 100 ns between laser excitation (266 nm; 10 mJ) and $\pi/2$ microwave pulse. The spectra display a strong absorption peak due to e$^-_{aq}$ ($g = 2.000$) and multiline contributions from the neutral phenoxyl radicals. The latter exhibit a low-frequency (high-field) absorption/high-frequency (low-field) emission (A/E) CIDEP pattern with the inversion point at the e$^-_{aq}$ resonance position.

The multi-line spectra were simulated with the *g* values and hyperfine coupling constants listed in Table 1. The values of the parameters are in good agreement with those reported previously for these phenoxyl radicals.[25,26] It is noted that the study of the tyrosyl radical by Sealy et al.[26] demonstrated that the room-temperature spectrum of this radical is affected by hindered rotation around the C−C bond linking the phenoxyl radical to the amino acid moiety. The resulting line broadening of some resonance peaks near the center of the spectrum make it appear as if only one of the methylene protons contributes to the hyperfine splitting (in the simulation mentioned above a(1H) = 1.506 mT). Spectra recorded at higher temperatures show that in fact both protons contribute with $a(2H) \approx 0.754$ mT.

Measurements with a range of delay time settings (10 ns to 10 μs) established that the signals from the phenoxyl radicals and e$^-_{aq}$ develop with a rate controlled by the instrument response time ($k_f \approx 4 \times 10^7$ s^{-1}). The decay of the e$^-_{aq}$ resonance peak is exponential with rate $k_d = 7.0 \times 10^5$ s^{-1}. The A/E spin polarization pattern is maintained over the entire time range that signals can be observed and corresponds to that found in earlier studies.[17−19] A change in excitation wavelength from 193 to 266 nm to 308 nm, whereas changing the overall intensity of the spectra did not affect the spin polarization pattern or the relative intensities of the signal contributions from the two paramagnetic species.

In the spectra of the phenoxyl radicals, resonance peaks turn from absorption to emission at the position of the e$^-_{aq}$ resonance (ν_e) (cf. Figure 1). This establishes that the spin state development in the radical pair, [PhO$^{\bullet}\cdots$ e$^-_{aq}$], is the dominant source of CIDEP. However, the integrals of the spectra presented in the insets of Figure 1 show that there is a net absorption signal contribution as well. For phenol and *p*-cresol the contributions amount to about 25 and 9%, respectively, of the maximum signal intensity and is not affected significantly by a change in excitation wavelength (193, 266, 308 nm). In the case of the tyrosyl radical, the net absorption contribution appears more substantial. However, this is ascribed to an instrumental artifact that is linked to the selective line broadening[26] referred to earlier. In the time-domain spectrum, signal contributions from the broad peaks decay to a significant extent during the deadtime of the instrument. This leads to an attenuation of the corresponding peaks in the frequency domain spectrum. These

TABLE 1: Hyperfine Coupling Constants and *g* Values of Free Radicals Generated by Pulsed-laser Excitation of Alkaline Solutions of Phenol, *p*-Cresol, and Tyrosine[d]

	phenoxyl	p-cresyl	tyrosyl
a_H (mT)	2H: 0.662 (0.660)[a] 2H: 0.181 (0.185)[a] 1H: 1.018 (1.025)[a]	2H: 0.610 (0.610)[a] 2H: 0.140 (0.140)[a] 3H: 1.258 (1.270)[a]	2H: 0.621 (0.620)[b] 2H: 0.150 (0.150)[b] 1H: 0.038 (0.035)[b] 1H: 1.506 (1.505)[b,c]
g	2.0040 (2.0046)[a]	2.0040 (2.0043)[a]	2.0042 (2.0046)[b]

[a] Ref 25. [b] Ref 26. [c] Sum of hyperfine couplings of two inequivalent protons (see text). [d] Literature values are given in parentheses.

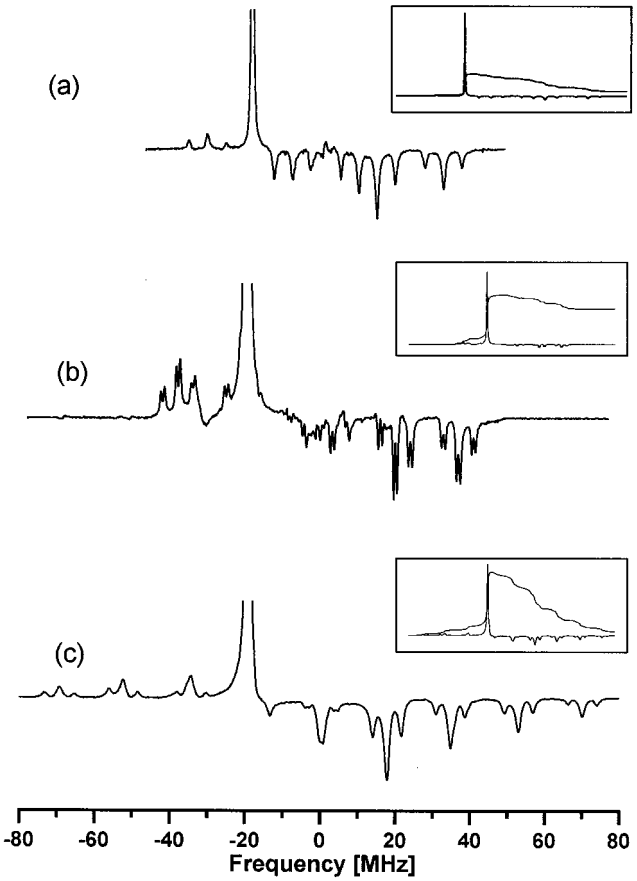

Figure 1. FT-EPR spectrum given by an aqueous solution (pH 11, 10^{-2} M) of (a) phenol, (b) tyrosine, and (c) p−cresol. Excitation wavelength 266 nm (10 mJ), 100 ns delay between microwave and laser pulses. Absorption peaks point up, emission peaks down. The insets show the relative amplitudes of the resonance peaks and the integrals of the spectra.

broad peaks are positioned in the, emissive, center of the spectrum so that the integration of the entire spectrum will show an excess absorption signal contribution. A measurement carried out at 60 °C, where the fast rotation limit is approached[26] and the line broadening effect has virtually vanished, indeed showed that the net absorption signal contribution had practically disappeared.

A quantitative analysis establishes that for short delay times ($\tau_d \approx 100$ ns) the integrated intensity (I_n) of each hyperfine peak in the spectra of the phenoxyl radicals divided by the degeneracy of the nuclear spin state associated with the resonance (d_n) is given by $I_n/d_n = P(|\nu_n - \nu_e|)^{1/2} + A$. Here, ν_n denotes the peak position, P is a proportionality constant ($P <$ 0 for $\nu_n < \nu_e$ and > 0 for $\nu_n > \nu_e$), and A represents the net absorption contribution. Figure 2 displays a fit of peak intensities based on this equation for the case of the free radical given by phenol. The dotted line in the figure marks the signal intensity versus frequency-offset dependence when A is set equal to zero and illustrates that the net absorption contribution barely exceeds the noise level. The $(|\nu_n - \nu_e|)^{1/2}$ dependence constitutes unequivocal evidence of a ST_0 RPM CIDEP signal contribution.[21]

3.2. Electron Scavenging by NO_3^-. Addition of KNO_3 to the phenolate solutions (pH 11) causes some interesting changes in the FT-EPR spectra. Figure 3 illustrates the effect of the presence of increasing amounts of NO_3^- on the spectra obtained at short delay time (100 ns) for solutions of phenol (pH 11).

At low concentration, $[NO_3^-] < 10^{-2}$ M, the spectra display

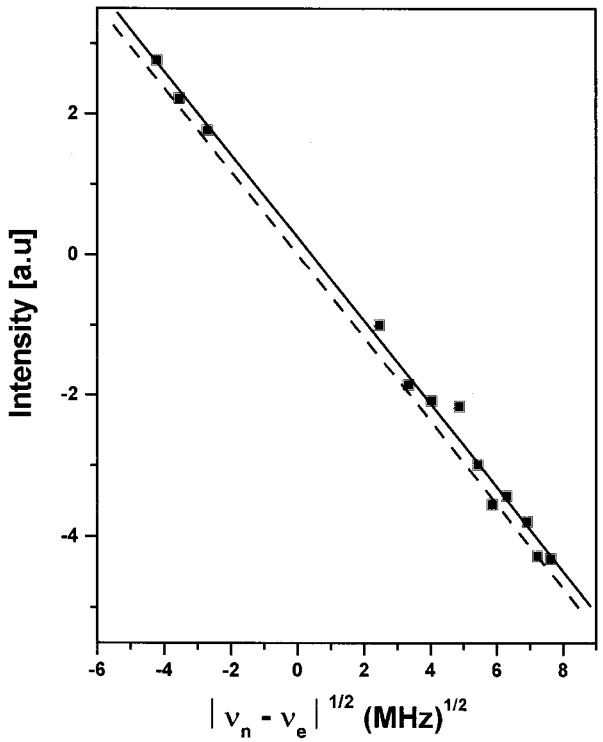

Figure 2. Plot of intensities of the PhO• resonance peaks in the spectrum given in Figure 1a (pH 11, delay 100 ns) versus the square root of the frequency offset from the e_{aq}^- resonance (see text for details). The dotted line marks the dependence of intensity on square root of frequency offset in the absence of the net absorption contribution.

three additional resonance peaks all in absorption and with about equal intensity. A measurement of the time evolution of signal intensities with $[NO_3^-] = 5 \times 10^{-4}$ M (cf. Figure 4a) shows that the three-line signal grows in at the expense of the resonance due to the hydrated electron. A least-squares fit of the data points (see Section 4 for details) gives a decay rate of the e_{aq}^- signal and a rate of three-line signal growth of 8.5×10^6 s^{-1}. At its maximum, the integrated intensity of the three-line signal matches the maximum in the intensity profile of the e_{aq}^- peak.

From these experimental data, it can be concluded that the three-line signal is due to the NO_3^{2-} radical formed in the reaction

$$NO_3^- + e_{aq}^- \rightarrow NO_3^{2-} \qquad (2)$$

The measured hyperfine splitting (a(N) = 4.33 mT) and g value (2.0045) are in reasonable agreement with values reported for this species in solids[27] and closely match those reported recently for NO_3^{2-} generated in liquid aqueous solution in a reaction of e_{aq}^- (produced by pulse radiolysis) with nitrate ions.[28] From the increase in the rate of decay of the e_{aq}^- signal upon addition of 5×10^{-4} M NO_3^- (cf. Figure 4a), it can be deduced that the rate constant of the electron scavenging reaction is 1.6×10^{10} $M^{-1}s^{-1}$. This value is in good agreement with published values of the rate constant of reaction 2.[10,29]

As the nitrate concentration is increased, the signal due to the hydrated electron is attenuated because of the increase in the rate of reaction 2. For $[NO_3^-] \geq 10^{-2}$ M, all e_{aq}^- generated in the photoionization step reacts in the interval between microwave pulse and FID acquisition (the instrument deadtime amounts to ~100 ns) so that it no longer gives a signal contribution. Even so, *the A/E polarization pattern in the spectra of the phenoxyl radicals remains centered around the* e_{aq}^-

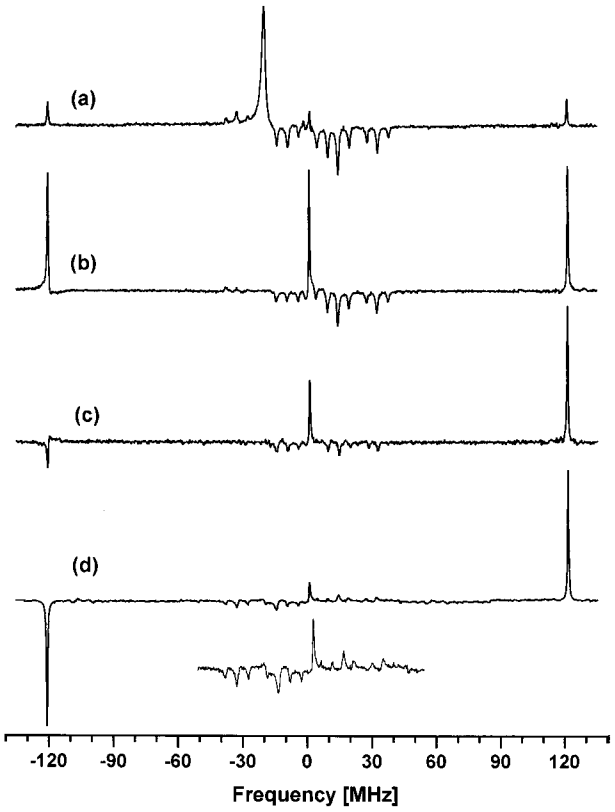

Figure 3. FT-EPR spectra given by aqueous solutions (pH 11) of phenol (10^{-2} M) for NO^{3-} concentrations of: (a) 5×10^{-4} M, (b) 9×10^{-3} M, (c) 5×10^{-2} M, and (d) 0.2 M. Excitation wavelength 266 nm (10 mJ), 100 ns delay between microwave and laser pulses. Absorption peaks point up, emission peaks down.

resonance frequency for NO_3^- *concentrations well above* 10^{-2} M *(cf. Figure 3c). This establishes unambiguously that* NO_3^{2-} *is formed by* e_{aq}^- *capture and not by oxidative quenching of excited phenolate.* As long as $[NO_3^-] \leq 10^{-2}$ M, for short delay times the three NO_3^{2-} resonance peaks are of equal intensity and in absorption, reflecting the spin polarization captured from e_{aq}^-.

As shown in Figure 3, the spin polarization pattern changes dramatically when the nitrate concentration is increased to the point where the rate of electron scavenging becomes of the order of 10^9 s^{-1} or higher. For short delay time settings the signals from $PhO^\bullet$ and NO_3^{2-} acquire an E/A signal contribution. With $[NO_3^-] = 0.2$ M (Figure 3d), the transition from E to A has shifted to the center of the spectrum for both radicals.

The striking difference in time evolution of the intensity of the NO_3^{2-} resonance peaks for $[NO_3^-] = 5 \times 10^{-4}$ M and 0.2 M is illustrated in Figures 4 and 5. It is noted that whereas the spin polarization pattern displays a pronounced concentration effect for $\tau_d < 1$ μs, for longer delay times, the three-line signal gradually develops A/E polarization at both low and high nitrate concentrations.

The delay-time dependence of the intensities of the resonance peaks due to e_{aq}^- and NO_3^{2-} for $[NO_3^-] < 10^{-3}$ M can be accounted for in terms of the following model: (1) Photoionization (instantaneous on the time scale of the measurements) followed by (2) an electron scavenging reaction in which NO_3^{2-} is formed with retention of the spin polarization of e_{aq}^-, and (3) a subsequent back electron-transfer reaction generating A/E polarization (F-pair CIDEP[20])

$$NO_3^{2-} + PhO^\bullet \leftrightarrow [NO_3^{2-} \cdots PhO^\bullet] \xrightarrow{k_{2d}} NO_3^- + PhO^- \quad (3)$$

The signal intensity of a given hyperfine peak ($M = -1$, 0, $+1$) due to NO_3^{2-} is proportional to the difference in population of the β and α electron spin states, $I_M = a(N_M^\beta - N_M^\alpha)$. According to the model, the time dependence of I_M then is given by

$$\frac{dI_M}{d_t} = \frac{I_{e_{aq}^-}(0)}{3} k_f' \exp(-k_f' t) - T_1^{-1}\left[I_M - I_{eq}\frac{NO_3^{2-}(t)}{3}\right] - k_{2d} PhO^\bullet(t)\left[I_M + I_M^{FP}\frac{NO_3^{2-}(t)}{3}\right] \quad (4)$$

In this equation, the first term represents the formation of spin polarized NO_3^{2-} with pseudo-first-order rate constant $k_f' = k_f[NO_3^-]$. The second term stands for spin−lattice relaxation to thermal equilibrium (I_{eq}). The third accounts for generation of F-pair spin polarization (with the condition that $I_{+1}^{FP} = -I_{-1}^{FP}$, $I_0^{FP} = 0$) as a result of the back electron-transfer reaction. It is assumed that electron scavenging is fast compared to spin−lattice relaxation of e_{aq}^-.

The solid lines in Figure 4a represent the result of a simultaneous least-squares analysis of the time profiles of the four resonance peaks using the numerical solution of 4). The analysis gave the following values for the parameters: $k_f' = 8.5 \times 10^6$ s^{-1}, $T_1 = 0.68$ μs, k_{2d} $[PhO^\bullet]_0 = 1.8 \times 10^{-5}$ s^{-1}, and $|I_{+1}^{FP}| = 25$ I_{eq}.

At high nitrate concentration (>0.1 M) the spin polarization pattern in the spectra (cf. Figures 3d and 5b) is dominated by RPM CIDEP generated by $[PhO^\bullet \cdots NO_3^{2-}]$. The rate of NO_3^{2-} signal growth in this case is instrument controlled. The time profiles of the intensities of the three hyperfine components in the spectrum of NO_3^{2-} for $\tau_d > 70$ ns were analyzed using the last two terms in eq 4) with the condition that $I_{+1}^{FP} = -I_{+1}^{FP}$, $I_0^{FP} = 0$. The analysis gave $T_1 = 0.63$ μs, $k_{2d}[PhO^\bullet]_0 = 4.5 \times 10^{-5}$ s^{-1}, and $|I_{+1}^{FP}| = 16$ I_{eq}. The polarization with which NO_3^{2-} is "born" is found to be $|I_{+1}| = 14$ I_{eq}, $|I_0| = 1.7$ I_{eq}, and $|I_{-1}| = 10$ I_{eq}. The solid lines in Figure 4b represent the result of the least-squares fit.

4. Discussion

In the absence of nitrate, the dominant source of spin polarization displayed in the spectra given by alkaline solutions of phenol, tyrosine, and *p*-cresol is the spin state development in the radical pair $[PhO^\bullet \cdots e_{aq}^-]$. The reversal of the polarization pattern from A/E to E/A upon addition of nitrate (cf. Figures 3 and 5) must be due to RPM CIDEP generated by the radical pair $[PhO^\bullet \cdots NO_3^{2-}]$. In the following, the question of whether the effect reflects a change in spin state of the excited-state precursor of these radical pairs or a change in sign of the exchange interaction J will be addressed. In addition, the discussion deals with what the observed CIDEP effects tell us about the spin state with which the pairs are born.

At low nitrate concentration ($<10^{-3}$ M), the sequence of reaction steps that accounts for the observed spin polarization and time evolution of signal intensities is the following; (i) formation of the radical pair $[PhO^\bullet \cdots e_{aq}^-]$, (ii) cage escape of free radicals, (iii) scavenging of e_{aq}^- by NO_3^-. The analysis of the time profiles of the intensity of the spectrum from NO_3^{2-} and of the e_{aq}^- resonance peak (cf. Figure 4a) establishes that the kinetics of generation of the three-line signal matches that of the decay of the e_{aq}^- signal. In addition, the intensity of the

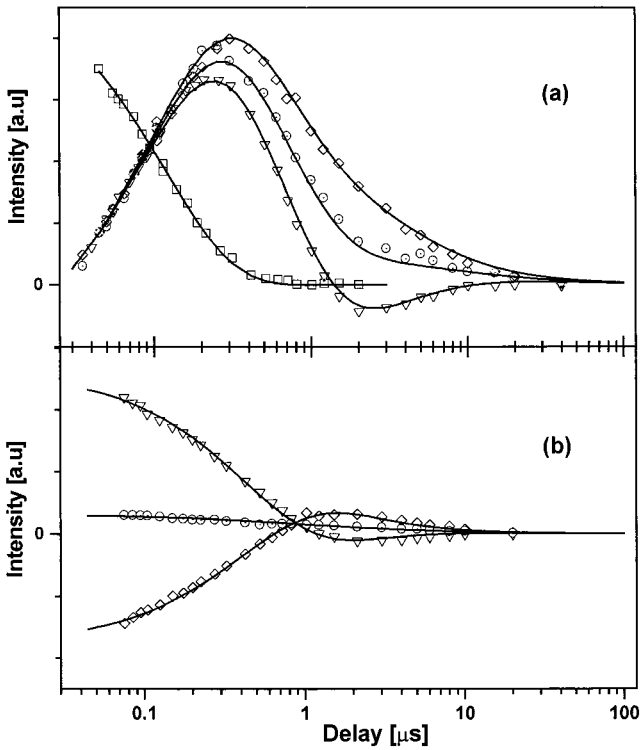

Figure 4. (a) Delay-time dependence of the intensities of e_{aq}^- (□) and NO_3^{2-} resonance peaks ((▽) M = +1; (⊙) M = 0; (◇) M = −1), given by aqueous solutions (pH 11) of phenol (10^{-2} M) and NO_3^- (5 × 10^{-4} M). (b) Delay−time dependence of the intensities of NO_3^{2-} resonance peaks ((▽) M = +1; (⊙) M = 0; (◇) M = −1) given by aqueous solutions (pH 11) of phenol (10^{-2} M) and NO_3^- (0.2 M). The solid lines represent the results of a least−squares fit of the data points using eq 4 (see text for details).

NO_3^{2-} spectrum at ∼300 ns equals that of the e_{aq}^- peak at 50 ns. It can be concluded, therefore, that direct electron transfer from singlet or triplet excited-state phenolate to nitrate does not play a role in NO_3^{2-} formation when $[NO_3^-] < 10^{-3}$ M. That electron-transfer quenching involving the singlet excited state of phenolate does not play a role under these conditions may be due to the short lifetime of $^1PhO^-$*.[5,10] That there is no evidence of $^3PhO^-$* quenching as a source of NO_3^{2-} could indicate that this is an uphill process. It may also signify that the quantum yield of triplet formation is low or that the triplet lifetime is short.[3]

The radical pair [PhO•··· NO_3^{2-}], which becomes the transient intermediate as the nitrate concentration is increased, can be formed via two routes: (1) photoionization of PhO^- followed by electron scavenging during the lifetime of [PhO•··· e_{aq}^-]

$$[PhO^{\bullet}\cdots e_{aq}^-] + NO_3^- \rightarrow [PhO^{\bullet}\cdots NO_3^{2-}] \qquad (5)$$

or (2) electron-transfer quenching of singlet or triplet excited-state phenolate

$$PhO^-* + NO_3^- \rightarrow [PhO^{\bullet}\cdots NO_3^{2-}] \qquad (6)$$

The following considerations lead to the conclusion that reaction 5 must be the route responsible for the observed change in polarization pattern.

Photoionization is an ultrafast process[10−16] that occurs on a time scale that is short compared to that in which electron-transfer quenching of PhO^-* (reaction 6)) can occur. Because the phenolates have an appreciable photoionization quantum yield (0.23−0.33 for phenol[5,10]), NO_3^{2-} formation must occur to a significant extent, if not exclusively, as a result of the e_{aq}^- scavenging reactions 2) and/or 5). In fact, in the picosecond study of the photoionization of phenolate by Mialocq et al.,[10] the characteristic absorption band of e_{aq}^- could still be observed in a solution containing 0.5 M NO_3^-. Under those conditions, the half-life of e_{aq}^- is reduced to 63 ps as a result of electron capture by nitrate.[10] Because the lifetime of [PhO•··· e_{aq}^-] in the absence of NO_3^- is expected to be of the order of some nanoseconds, the electron scavenging reaction must occur prior to dissociation of this radical pair. (It is relevant to note that Jortner et al.[11] found evidence for such a cage-scavenging process in the reaction of e_{aq}^-, produced by photoionization of phenolate, with N_2O.) The radical pair spin state evolution generating ST_0 RPM CIDEP occurs over a time span of tens of nanoseconds.[21,30,31] Hence, if reaction 5 is responsible for the change in polarization pattern, the pattern should start to change at the point where the cage-scavenging reaction reduces the [PhO•··· e_{aq}^-] lifetime to a few nanoseconds. Given that scavenging rate constant is ∼2 × 10^{10} $M^{-1}s^{-1}$, this point will be reached when $[NO_3^-] > 10^{-2}$ M. The NO_3^{2-} signal indeed starts to display a [PhO•··· NO_3^{2-}] CIDEP contribution for $[NO_3^-]$ = 2 × 10^{-2} M and this contribution becomes dominant when $[NO_3^-] = 5 \times 10^{-2}$ M as is illustrated in Figure 3c.

Although the experimental data are consistent with the cage-scavenging (reaction 5) route of [PhO•··· NO_3^{2-}] formation, this is not the case for the alternative route. At a nitrate concentration in the range of 1 × 10^{-2} to 5 × 10^{-2} M, electron-transfer quenching of $^1PhO^-$* at best must be a minor process compared to electron scavenging from [PhO•··· e_{aq}^-] because the lifetime of the singlet excited state of phenolate is ≤0.3 ns.[5,10] This leaves electron-transfer quenching of triplet phenolate as a possible source of NO_3^{2-}. Transient optical absorption spectra of phenol in neutral aqueous solution show an absorption band due to ^3PhOH* (τ_T = 3.3 μs); however, spectra taken at pH > 10 do not show a band due to $^3PhO^-$*.[3] Apparently, the quantum yield of triplet state formation is very low in basic solution or the triplet state lifetime is very short (≤10^{-10} s). In either case, electron-transfer quenching of phenolate triplets cannot be a significant path of NO_3^{2-} formation.

The relative intensities of e_{aq}^- and NO_3^{2-} signal intensities are consistent with the conclusion that electron scavenging remains the main route of NO_3^{2-} formation even at high nitrate concentrations. Assuming that the lifetimes and $|J|$ values are similar for the two radical pairs, the integrated intensities of the resonance peaks given by e_{aq}^- and NO_3^{2-}, normalized to account for the dependence of signal intensity on the square root of the frequency offset from the center of the $PhO^{\bullet}$ spectrum, should be equal.[20,21] For the samples phenol (10^{-2} M)/NO_3^- (0.2 M) and tyrosine (10^{-2} M)/NO_3^- (0.2 M) the ratios of the normalized intensities were found to be 1.1 and 1.2, respectively. It is noted that this relationship does not necessary hold if the route of formation of NO_3^{2-} formation switches from electron scavenging to excited-state electron transfer. Even if both processes involve the singlet excited state, the quantum yields can differ because photoejection of electrons can take place in competition with relaxation processes that produce the thermalized excited state from which electron transfer may occur.[5]

It must be concluded that the reversal of the polarization pattern as the nitrate concentration is increased is due to a switch in the spin sorting process taking place when [PhO•··· e_{aq}^-] is transformed into [PhO•··· NO_3^{2-}]. Because this switch is not due to a change in spin multiplicity with which the radical pairs

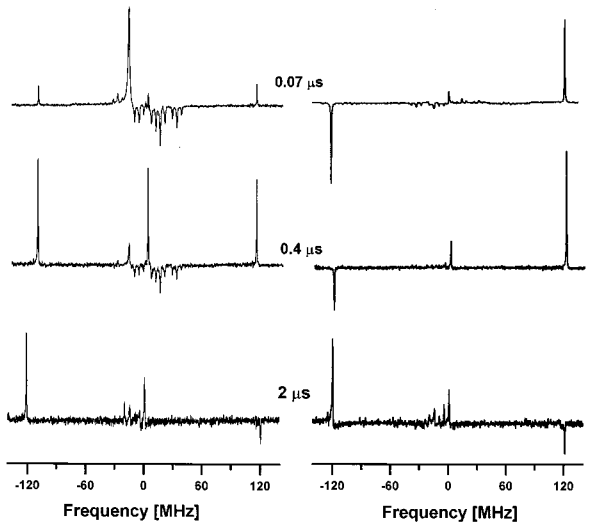

Figure 5. FT-EPR spectra for different delay times between laser and microwave pulses, given by aqueous solutions (pH 11) of phenol (10^{-2} M) with 5×10^{-4} M (left) and 0.2 M (right) NO_3^-.

are born, it must stem from a change in sign of the exchange interaction *J*.

Finally, the spin multiplicity with which these radical pairs are "born" can be deduced from the evolution of the spectra given by phenol/NO_3^- solutions at longer delay times. Figures 4 and 5 show that the E/A pattern in the spectra of $PhO^\bullet$ and NO_3^{2-} eventually evolves into an A/E pattern. As noted earlier, this phenomenon reflects RPM CIDEP generated by back electron transfer. Encounters in which the radical pairs are formed in the singlet state lead to reaction. This leaves triplet state pairs that can dissociate to yield free radicals with spin polarization characteristics of CIDEP generated by triplet state radical pairs (F-pair RPM CIDEP[20]). Assigning the A/E pattern observed at longer delay times to CIDEP generated by $^3[PhO^\bullet\cdots NO_3^{2-}]$, the E/A pattern at early times must be attributed to formation of the singlet radical pair $^1[PhO^\bullet\cdots NO_3^{2-}]$. The exchange interaction in this pair must by negative as is usually found in radical pairs formed by electron transfer or bond homolysis.[20]

As noted above, formation of $^1[PhO^\bullet\cdots NO_3^{2-}]$ occurs primarily via reaction 5 *so that the precursor pair*, $[PhO^\bullet\cdots e_{aq}^-]$, *must be produced by singlet excited-state photoionization and J in this pair must be positive.*

In a recent study by Kobori et al.,[22] it was reported that the sign of *J* in radical pairs, $^{1,3}[A^-\cdots D^+]$, generated by photoinduced electron transfer may depend on the free energy of the radical pair state relative to the localized singlet and triplet excited states, $[^1A^*\cdots D]$ and $[^3A^*\cdots D]$, and the ground state $[^1A\cdots D]$. In cases where the $^{1,3}[A^-\cdots D^+]$ state lies slightly above $[^3A^*\cdots D]$, CIDEP effects indicate that $J > 0$. This is attributed to stabilization of the triplet radical pair state by admixture with the localized triplet state.[22] In cases where the radical pair state lies well below the localized excited state it is expected that $J < 0$. The finding that $J > 0$ in $[PhO^\bullet\cdots e_{aq}^-]$ and becomes negative in $[PhO^\bullet\cdots NO_3^{2-}]$ appears to fit this interpretation. The energy of $[PhO^\bullet\cdots e_{aq}^-]$ is expected[17] to be close to that of $^3PhO^-{}^*$ and the electron scavenging reaction giving $[PhO^\bullet\cdots NO_3^{2-}]$ will lead to a significant lowering of the radical pair energy as evident from the high rate of electron scavenging.

In an earlier cw TREPR study, Jeevarajan and Fessenden[17] also concluded that photoionization involves a singlet excited state and that $J > 0$. These authors based their conclusion among other things on the finding that photoionization of phenolates gives rise to EPR spectra showing E/A polarization, whereas the spectra given by phenoxyl radicals and e_{aq}^- generated in independent steps by pulse radiolysis have an A/E pattern. In the latter case, spin polarization results from the spin state evolution in $^3[PhO^\bullet\cdots e_{aq}^-]$ F-pairs, in the former from $^1[PhO^\bullet\cdots e_{aq}^-]$ geminate-pairs formed in reaction 1. Clancy and Forbes, on the other hand, reported that photoionization of tyrosine in alkaline aqueous solution involves the triplet excited state.[18] Their conclusion is based on the finding that addition of the triplet quencher sorbic acid (0.6 M) to the solution results in the disappearance of the TREPR signal. However, photoionization is expected[10] to occur at a rate that far exceeds the rate of encounters between (triplet) excited tyrosinate and quencher. Therefore, it is unlikely that the quencher can have a significant effect on photoionization quantum yield. Instead its effect on the TREPR signal may be due to radical quenching reactions.

In the present study and in an earlier FT-EPR study,[19] of the photoionization of sesamol (3,4-methylenedioxyphenol) the spectra reveal a net absorption contribution in addition to the E/A signal contribution. In the case of phenol, *p*-cresol, and sesamol, this contribution amounts to only a small percentage (11−16%) of the overall signal intensity (cf. Figures 1 and 2). For tyrosine, the effect is more pronounced (28%), however, as pointed out in Section 3.1, this can be attributed to an instrumental effect caused by severe line broadening of selected lines in the tyrosyl spectrum.[26] The net absorption signal contribution was attributed[19] to spin polarization carried over from the triplet excited state of the phenolates and was taken as evidence of a photoionization mechanism involving the triplet excited state. It was proposed that the E/A polarization stemmed from the same reaction channel. Evidently, the present data do not support this interpretation. Instead the net absorption may point to a minor signal contribution from radicals generated via the triplet excited state. Alternatively, it may simply be a consequence of small errors in relative intensities of resonance peaks introduced by the routines used to generate the frequency domain spectra from the FIDs.

Previous optical studies[5] established that the photoionization quantum yield of phenols increases with increasing photon energy and that this is accompanied by a decrease in fluorescence. This was taken as evidence that electron ejection is a singlet excited-state process that occurs in competition with relaxation to the fluorescent state. The results of the present FT-EPR measurements are in accord with this interpretation.

Acknowledgment. Financial support for this work was provided by the Division of Chemical Sciences, Office of Basic Energy Sciences of the US Department of Energy (DE-FG02-84ER-13242).

References and Notes

(1) Feitelson, J.; Hayon, E. *J. Phys. Chem.* **1973**, *77*, 10.

(2) Feitelson, J.; Hayon, E.; Treinin, A. *J. Am Chem. Soc*. **1973**, *95*, 1025.

(3) Bent, D. V.; Hayon, E. *J. Am Chem. Soc*. **1975**, *97*, 2599.

(4) Zechner, J.; Köhler, G; Grabner, G.; Getoff, N. *Chem. Phys. Lett*. **1976**, *37*, 297.

(5) Grabner, G.; Köhler, G.; Zechner, J.; Getoff, N. *Photochem. Photobiol*. **1977**, *26*, 449.

(6) Köhler, G.; Getoff, N. *J. Chem. Soc., Faraday I* **1976**, *72*, 2101.

(7) Zechner, J.; Köhler, G.; Grabner, G.; Getoff, N. *Can. J. Chem*. **1980**, *58*, 2006.

(8) Grabner, G.; Köhler, G.; Zechner, J.; Getoff, N. *J. Phys. Chem*. **1980**, *84*, 3000.

(9) Grabner, G.; Köhler, G.; Marconi, G.; Monti, S.; Venuti, E. *J. Phys. Chem*. **1990**, *94*, 3609.
(10) Mialocq, J.; Sutton, J.; Goujon P. *J. Chem. Phys*. **1980**,*72*, 6338.
(11) Jortner, J.; Ottolenghi, M.; Stein, G. *J. Am. Chem. Soc.* **1963**, *85*, 2712.
(12) Goldschmidt, C.; Stein, G. *Chem. Phys. Lett*. **1970**, *6*, 299.
(13) Matsuzaki, A.; Kobayashi, T.; Nagakura, S. *J. Phys. Chem.* **1978**, *82*, 1201.
(14) Gauduel, Y.; Berrod, S.; Migus, A.; Yamada, N.; Antonetti, A. *Biochemistry* **1988**, *27*, 2509.
(15) Ghosh, H. N.; Palit, D. K.; Sapre, A. V.; RamaRao, K. V. S.; Mittal, J. P. *Chem. Phys. Lett.* **1993**, *203*, 5.
(16) Peon, J.; Hess, G. C.; Pecourt, J.-M. L.; Yuzawa, T.; Kohler, B. *J. Phys. Chem. A* **1999**, *103*, 2460.
(17) Jeevarajan, A. S.; Fessenden, R. W. *J. Phys. Chem*. **1992**, *96*, 1520.
(18) Clancy, C. M. R.; Forbes, M. D. E. *Photochem. Photobiol*. **1999**, *69*, 16.
(19) Bussandri, A.; van Willigen, H.; Nakagawa, K. *Appl. Magn. Res.* **1999**, *17*, 577.
(20) For a review of CIDEP effects and leading references see McLauchlan, K. A. In *Modern Pulsed and Continuous Wave Electron Spin Resonance*; Kevan, L.; Bowman, M. K., Eds.; Wiley: New York, 1990; pp 285−364.
(21) Adrian, F. *J. Chem. Phys.* **1971**, *54*, 3918.
(22) Kobori, Y.; Sekiguchi, S.; Akiyama, K.; Tero-Kubota, S. *J. Phys. Chem. A* **1999**, *103*, 5416.
(23) Levstein, P. R.; van Willigen, H. *J. Chem. Phys*. **1991**, *95*, 900.
(24) de Beer, R.; van Ormondt, D. In *Advanced EPR: Applications in Biology and Biochemistry*; Hoff, A. J., Ed.; Elsevier: Amsterdam, 1989; pp 135−173.
(25) Dixon, W. T.; Murphy, D. *J. Chem. Soc., Perkin Trans. 2* **1976**, 1823.
(26) Sealy, R. C.; Harman, L.; West, P. R.; Mason, R. P. *J. Am. Chem. Soc.* **1985**, *107*, 3401.
(27) Rustgi, S. N.; Box, H. C. *J. Chem. Phys.* **1973**, *73*, 4763.
(28) Fessenden, R. W.; Meisel, D. *J. Am. Chem. Soc.* **2000**, *122*, 3773.
(29) Anbar, M.; Bambeneck, M.; Ross, A. B. *Selected Specific Rates of Reactions of Transients from Water in Aqueous Solution. I. Hydrated Electron*, Natl. Stand. Ref. Data Ser.; Natl. Bur. Stand: 1973; 43.
(30) Shkrob, I. A. *Chem. Phys. Lett.* **1996**, *264*, 417.
(31) Adrian, F. J. *Chem. Phys. Lett.* **1997**, *272*, 120.